Catena 274 (2026) 110529

Contents lists available at ScienceDirect

Catena

journal homepage: www.elsevier.com/locate/catena

Drainage reorganization driven by strike-slip faulting along the Xiaojiang Fault, Southeastern Tibet: A new explanation for geohazards in the Xiaojiang River watershed

Yijia Ye [a], Xibin Tan [a,b,*], Dongri Song [a,b]

[a] Key Laboratory of Mountain Hazards and Engineering Resilience, Institute of Mountain Hazards and Environment, Chinese Academy of Sciences, Chengdu 610213, China

[b] Joint Laboratory of Mountain Hazard Prevention and Mitigation, Institute of Mountain Hazards and Environment, Chinese Academy of Sciences, Chengdu 610213, China

ARTICLE INFO

Keywords:
Drainage reorganization
Drainage-divide migration
Xiaojiang Fault
Geohazards
Jiangjia Ravine
Southeastern Tibet

ABSTRACT

The Xiaojiang River, located at the southeastern margin of the Tibetan Plateau, is one of the world's most landslide- and debris-flow-prone regions. The main trunk of the Xiaojiang River closely follows the Xiaojiang Fault, a major block-boundary fault characterized by sinistral strike-slip motion. However, it is still unclear how the strike-slip faulting governs the long-term drainage evolution of the Xiaojiang River and, in turn, influences the geohazards within the Xiaojiang River watershed. Here we investigate the drainage evolution of the Xiaojiang River using high-resolution topography and quantitative geomorphic analyses, with a particular focus on drainage-divide migration and river capture. Our results reveal that most tributaries within the Xiaojiang River watershed are undergoing catchment expansion, primarily driven by fault-induced bedrock weakening. The expansion of the Xiaojiang River watershed further promotes soil erosion and landslides in the basin. We further identify a river-capture event controlled by the strike-slip faulting, which caused a ~ 400 m drop in the local base level and likely contributed to the exceptional concentration of debris flows in the Jiangjia Ravine. These findings demonstrate that tectonically driven drainage reorganization is an important control on the spatial distribution of regional geohazards. Incorporating dynamic drainage evolution into hazard-assessment frameworks is therefore essential for improving long-term risk mitigation in tectonically active mountain belts.

1. Introduction

River networks are dynamic in response to the combined influences of tectonic activity, climate change, and lithologic heterogeneity (Bonnet, 2009; Willett et al., 2014; Duffy et al., 2015; Harel et al., 2019; Zondervan et al., 2020; Zhang et al., 2022). Through processes such as progressive drainage-divide migration and discrete river captures, river network reorganization modifies channel network topology and redistributes drainage area (Bishop, 1995; Willett et al., 2014; Beeson et al., 2017; Whipple et al., 2017; Chen et al., 2021a; Stokes et al., 2023; Bian et al., 2025). These adjustments exert an important control on spatial patterns of stream power and river incision, thereby regulating sediment production and hillslope processes, including mass wasting and slope failure (Burbank et al., 1996; Montgomery and Brandon, 2002; Ng, 2006; Reinhardt et al., 2007; Larsen and Montgomery, 2012; Blöthe et al., 2015). River capture, in particular, can produce rapid geomorphic responses by imposing abrupt base-level drop that accelerate upstream incision, enhance basin-wide erosion, and destabilize hillslopes (Bishop, 1995; Yanites et al., 2013; Fan et al., 2018; Baynes et al., 2022; Bian et al., 2025). Such long-term landscape adjustments may precondition mountain regions to heightened susceptibility to landslides and debris flows (Gallen et al., 2011; Larsen and Montgomery, 2012), complementing the effects of short-term triggers such as rainfall and earthquakes (Lan et al., 2004; Umar et al., 2014; Chen et al., 2021b; Zou et al., 2022; Li et al., 2022; Sun et al., 2022; Morales et al., 2023; Pei et al., 2023; Qi et al., 2025). However, the extent to which drainage-basin evolution governs the spatial distribution and persistence of geohazards remain under-investigated,

* Corresponding author at: Key Laboratory of Mountain Hazards and Engineering Resilience, Institute of Mountain Hazards and Environment, Chinese Academy of Sciences, Chengdu 610213, China.
E-mail address: tanxibin@imde.ac.cn (X. Tan).

https://doi.org/10.1016/j.catena.2026.110529
Received 12 May 2026; Received in revised form 18 July 2026; Accepted 17 August 2026

especially in tectonically active mountain regions.

The Xiaojiang River, located at the deeply incised southeastern margin of the Tibetan Plateau, provides an exceptional natural laboratory for investigating these interactions. The river flows generally northward into the Jinsha River and traverses terrain characterized by extreme relief, highly fractured bedrock, and frequent seismic activity (Fig. 1) (Shen et al., 2003; Hu et al., 2011; Hu et al., 2021; Zhang et al., 2025). The Xiaojiang River watershed is widely recognized as one of the world's most severely affected regions by frequent and catastrophic landslides and debris flows (e.g., Jiangjia Ravine), which exert the persistent threat to downstream communities, infrastructure, and ecosystems (Scott and Wang, 2004; Hu et al., 2021; Song, 2023; Zhang et al., 2025; Wei et al., 2025). This severe hazard environment motivates an investigation that extends beyond immediate trigger mechanisms toward the deeper, long-term geomorphic processes that regulate mass wasting.

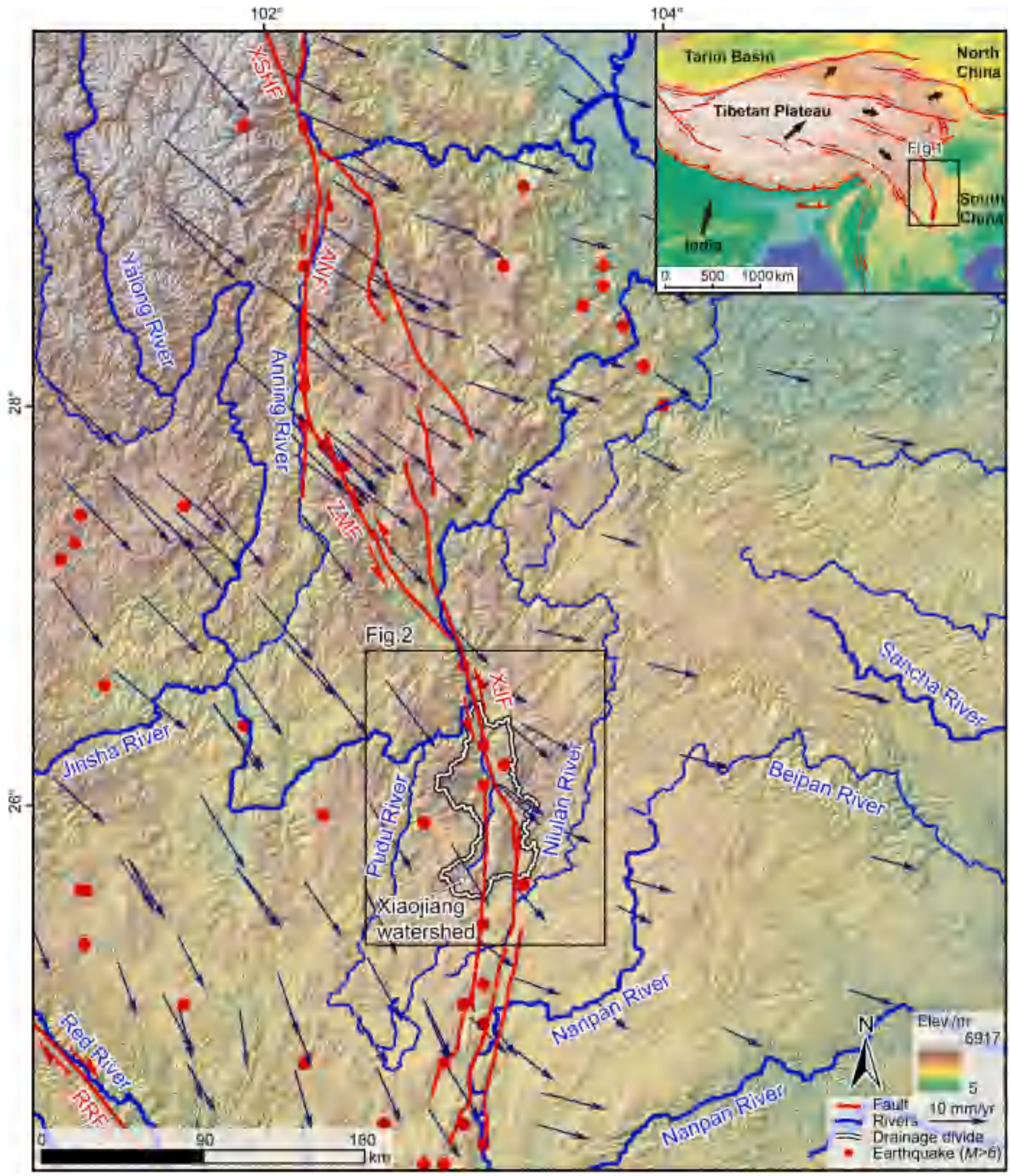

Fig. 1. Topographic and tectonic background map of the study area. The arrows show the GPS velocities field (Wang and Shen, 2020). White line bordered in black represents the drainage divide surrounding the Xiaojiang River watershed. Red lines represent the main active faults. Blue lines show the main rivers. The topography data (DEM) is obtained from the Alaska Satellite Facility Data Search (https://search.asf.alaska.edu/). ANF: Anninghe Fault; RRF: Red River Fault; XJF: Xiaojiang Fault; XSHF: Xianshuihe Fault; ZMF: Zemuhe Fault. (For interpretation of the references to colour in this figure legend, the reader is referred to the web version of this article.)

The Xiaojiang Fault, a sinistral strike-slip fault accommodating the southeastward extrusion of the Tibetan Plateau, cuts directly through the Xiaojiang River watershed (Wang et al., 1998; Wang and Burchfiel, 2000; Shen et al., 2005; He and Oguchi, 2008; Wen et al., 2011; Bai et al., 2025; Zhang et al., 2026a). Strike-slip faulting can profoundly reorganize river networks by altering channel gradients, deflecting flow paths and promoting drainage capture and divide migration (Ouchi, 2005; Duvall and Tucker, 2015; Gray et al., 2018; Dascher-Cousineau et al., 2021; Tian and Lin, 2021; Zeng and Tan, 2023; Aránguiz-Rago et al., 2025). However, how the Xiaojiang Fault influences the long-term evolution of the Xiaojiang River watershed, and further impacts the regional geohazards remain under-investigated.

Recent advances in drainage-divide stability analysis provide a powerful tool for investigating drainage-basin evolution and its underlying controls (Willett et al., 2014; Whipple et al., 2017; Forte and Whipple, 2018; Zhou et al., 2022a; Ye et al., 2024a; Bian et al., 2024; Li et al., 2025). In this study, we first use χ-plots method to measure the stability of the primary and secondary drainage divides within the Xiaojiang River watershed (Zhou et al., 2022b). We then reconstruct the drainage evolution of the watershed and evaluate the relative roles of strike-slip faulting, tectonic uplift, climate, and lithologic variations in controlling this evolution. Finally, we examine the process-based relationship between long-term drainage reorganization and the spatial distribution of landslides, with the goal of clarifying how landscape dynamics influence regional geohazard patterns.

2. Regional setting

The Xiaojiang River, located at the southeastern margin of the Tibetan Plateau, is a major tributary of the Jinsha River, and flows from south to north, with elevations decreasing from approximately 2500 m in the headwater region to about 740 m at its confluence with the Jinsha River. Bedrock within the basin comprises a heterogeneous assemblage of volcanic, sedimentary, and metamorphic units (Fig. 2A). Exposed igneous rocks are dominated by calc-alkaline basalt, locally interlayered with clastic sedimentary strata, including sandstone and mudstone. Metamorphic rocks are primarily distributed along the northwestern margin of the basin and consist mainly of low- to medium-grade metasedimentary units, such as metaclastic rocks and slate. Sedimentary rocks are widely developed throughout the basin and consist predominantly of sandstone, mudstone, and limestone. Mean annual precipitation across the basin ranges from approximately 750 to 980 mm/yr (Fig. 2B).

The main trunk of the Xiaojiang River basically flows along the Xiaojiang Fault, which is characterized by left-lateral strike-slip motion (He et al., 1993; Song et al., 1998; Shen et al., 2003; He and Oguchi,

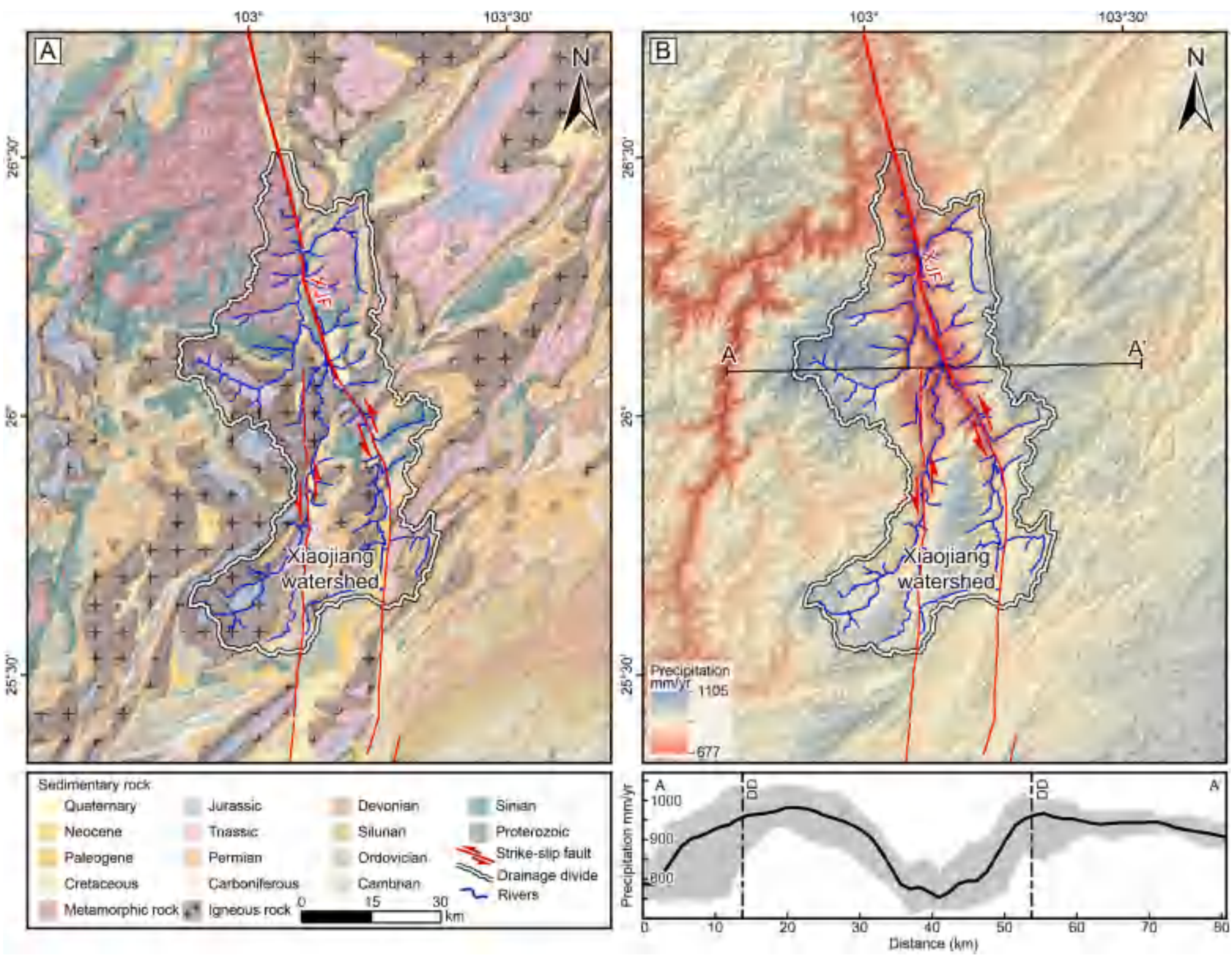

Fig. 2. (A) Geological map of the Xiaojiang River watershed and the surrounding area. (B) The distribution of mean annual precipitation. Data for the period of 1970–2000 are download from http://worldclim.org (Fick & Hijmans, 2017). A 30-km-wide swath profile (A-A') reveals that the Xiaojiang River watershed receives slightly less precipitation than the catchment to the east and is basically consistent with that to the west.

2008; Guo et al., 2021). The central segment of the Xiaojiang Fault is divided into eastern and western branches (Figs. 1 and 2). Geological investigations have estimated late Quaternary left-lateral slip rates of ~13–22 mm/yr along the Xiaojiang Fault system, with lower rates of ~6–10 mm/yr along the eastern branch of the central segment (He et al., 2002; Shen et al., 2003; He and Oguchi, 2008). Geodetic measurements indicate present-day left-lateral slip rates of ~7–10 mm/yr across the fault system (Shen et al., 2005; Wang et al., 2008; Wen et al., 2011; Wang and Shen, 2020). The Xiaojiang Fault exhibits high seismic activity and has generated numerous large historical earthquakes, including the 1733 Dongchuan earthquake (*M* 7.75) (Min et al., 1995; Ren, 2013; Wen et al., 2011; Guo et al., 2021). Owing to active tectonics, highly fractured bedrock, and relatively high precipitation, the Xiaojiang River watershed is recognized as a globally significant hotspot for debris flows and landslides (Wei et al., 2025; Zhang et al., 2025). The Jiangjia Ravine, a tributary within the watershed, exhibits a particularly high frequency of debris-flow activity (Cui et al., 2005; Zhuang et al., 2015; Chen et al., 2023). A total of 278 debris-flow events were documented in the Jiangjia Ravine between 1961 and 2024 (Wei et al., 2025).

3. Method

Cross-divide differences in erosion rates control drainage-divide migration (Whipple et al., 2017; Willett et al., 2014; Ye et al., 2024b). According to the stream-power incision model (Howard, 1994), erosion rate (E) is typically expressed in a generalized form (Kirby et al., 2003; Kirby and Whipple, 2012):

$$E = KA^m S^n \tag{1}$$

where K is erosion coefficient; A is upstream drainage area; S is channel gradient; m and n are the area exponent and slope exponent, respectively.

By integrating from a base level x_b to an observation point x in the upstream direction, a transformed elevation profile can be rewritten as (Perron and Royden, 2013):

$$z(x) = z(x_b) + \int_{x_b}^{x} \left(\frac{E(x)}{K(x)}\right)^{\frac{1}{n}} A(x)^{\frac{-m}{n}} dx \tag{2}$$

Eq. (2) can be simplified as:

$$z(x) = z_b + \left(\frac{E}{K}\right)^{\frac{1}{n}} \int_{x_b}^{x} \frac{dx}{A(x)^{\frac{m}{n}}} \tag{3}$$

To create the transformed river profile with length unit on both axes, Perron and Royden (2013) introduced a reference drainage area, A_0, to make the integrand dimensionless:

$$z(x) = z_b + k_{sn}(A_0)^{\frac{-m}{n}} \chi \tag{4}$$

with

$$k_{sn} = \left(\frac{E}{K}\right)^{\frac{1}{n}} = SA^{\frac{m}{n}} \tag{5}$$

$$\chi = \int_{x_b}^{x} \left(\frac{A_0}{A(x)}\right)^{\frac{m}{n}} dx \tag{6}$$

A plot of river channel elevation (z) versus integral quantity (χ) is commonly referred to as a χ plot (Perron and Royden, 2013; Willett et al., 2014). When A_0 is set to 1 m^2 and a uniform concavity index (m/n) is assumed, the slope of the χ plot corresponds to the normalized channel steepness (k_{sn}), which is positively and monotonically related to erosion rate (Wobus et al., 2006; Ouimet et al., 2009; Kirby and Whipple, 2012). River-pair χ plots, constructed from river channels on either side of a drainage divide, capture differences in χ-plots slope and, consequently, in k_{sn} across the divide, enabling assessment of divide stability (Zhou et al., 2022b). In applying the χ-plots method, selecting a high base level helps minimize the influence of spatial variations in uplift, thereby producing linear or quasi-linear river-pair χ plots suitable for comparison (Zhou et al., 2022b). Additionally, river pairs should be selected within similar lithologic units to ensure comparable erosion coefficients on both sides of the divide. Under these conditions, drainage divides are expected to migrate toward the side with larger χ values, which correspond to a lower χ-plots slope and lower k_{sn} (Willett et al., 2014; Zhou et al., 2022b).

In this study, drainage-divide stability was evaluated using the χ-plots method (Zhou et al., 2022b). A critical threshold drainage area (A_c) of 1×10^5 m^2, derived from the relationship between drainage area and local slope (Fig. S1), was applied to extract the drainage network from 12.5 m resolution ALOS digital elevation models. χ values were calculated using an A_0 of 1 m^2 and a concavity index of 0.45, which yields convergence of tributaries and trunk-stream profiles onto a common trend in the χ plots (Fig. S2) (Kirby and Whipple, 2012; Perron and Royden, 2013). River pairs were then selected from channels located on opposite sides of drainage divides, and average k_{sn} values were measured from the highest part of the χ plots (Zhou et al., 2022b). To quantify divide mobility, we computed the normalized cross-divide contrast in k_{sn} ($\Delta k_{sn}/\overline{k_{sn}}$), which serves as a metric for the magnitude and direction of potential divide migration (Bian et al., 2024; Ye et al., 2024a). In addition, sensitivity analyses were performed for the concavity index ($m/n = 0.35$, 0.45, and 0.55) to evaluate the reliability of the χ-plots results. All topographic analysis and drainage extraction were performed using the TopoToolbox (Schwanghart and Scherler, 2014), whereas χ-plots analysis was conducted using the Topographic Analysis Kit (TAK) (Forte and Whipple, 2019), an extension and integrated program based on TopoToolbox.

4. Results

To assess drainage-divide stability across the Xiaojiang River watershed, 36 pairs of opposing river channels were selected for χ-plots analysis (Figs. 3, S3&S4). Bedrock lithology was examined using regional geological map for each river pair in the vicinity of the corresponding drainage divide (Fig. S3). Bedrock lithologies are similar on both sides of most drainage divides, with only five river pairs crossing mapped lithologic boundaries (Fig. S3). Although lithologic contrasts occur within these five river cases, they do not affect the interpretation of divide migration directions (Fig. S3). Furthermore, sensitivity analyses demonstrate that variations in concavity index ($m/n = 0.35$, 0.45, and 0.55) do not alter the inferred drainage-divide stability (Fig. S5).

χ-plots analysis of the 36 river pairs indicates that only 3 pairs show stable drainage divides, whereas the remaining 33 exhibit active and ongoing divide migration (Figs. 3 and S4). Along the eastern flank of the basin, χ plots indicate that the Xiaojiang River watershed is progressively expanding eastward into the Yili River watershed. In contrast, the western flank exhibits more complex patterns of divide migration: the headwater region of the Xiaojiang River watershed shows evidence of drainage contraction, whereas the central and downstream sections are expanding westward into the Pudu River watershed. Overall, these results indicate progressive outward expansion of the Xiaojiang River watershed (Fig. 3).

To further investigate the drainage-divide stability along the eastern flank, we conducted a detail comparison of topographic characteristics and geomorphic indices, including k_{sn} and χ (Fig. 4). High-resolution satellite imagery from Google Earth, together with a topographic swath profile, reveals pronounced morphological asymmetry across the divide (Fig. 4B and D). Specifically, the western side (within the Xiaojiang River watershed) exhibits markedly steeper slopes and more deeply incised channels than the eastern side (Fig. 4). This topographic contrast is also reflected in the spatial distributions of key geomorphic parameters (Fig. 4A–C). The k_{sn} map and four representative river-pair χ

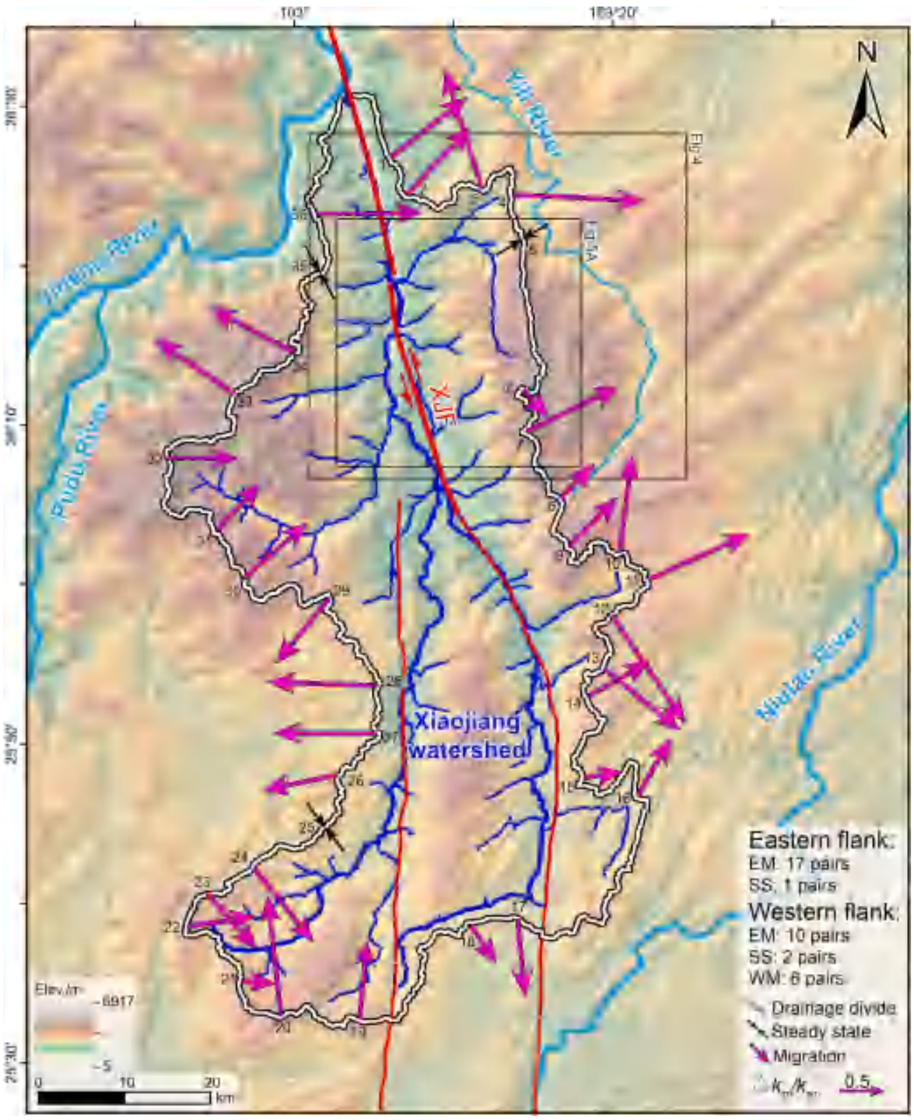

Fig. 3. Results of the drainage-divide stability obtained by χ-plots analysis. The vectors in magenta represent the drainage-divide migration direction and normalized cross-divide difference in k_{sn} ($\Delta k_{sn}/\overline{k_{sn}}$). Black arrows represent the stable divides. The detailed results of the χ plots are provided in Supplementary Materials Fig. S1 and Table S1. Thirty-three river-pair χ plots show that the drainage divide is moving, while three river-pair χ plots show the drainage divide is stable. (For interpretation of the references to colour in this figure legend, the reader is referred to the web version of this article.)

plots consistently show higher k_{sn} values on the western side (Fig. 4B and C). These systematic cross-divide contrasts in topography, k_{sn}, and χ collectively suggest that the eastern flank of the Xiaojiang River watershed is actively expanding eastward into the Yili River watershed.

In addition to the basin-scale analysis, we evaluated the stability of drainage divides surrounding the Jiangjia Ravine, an interior tributary characterized by an exceptionally high frequency of debris flows relative to other parts of the Xiaojiang River watershed (Fig. 5A and B) (Wei et al., 2025). Analysis of eight χ plots reveals that in seven river pairs, the drainage divides are migrating outward, indicating that the Jiangjia Ravine is expanding its contributing area through headward erosion from adjacent basins (Fig. 5A and S6). Notably, regions located to the south of the Jiangjia Ravine, such as the Laobaidi Valley, show a markedly lower incidence of landslides and debris flows (Fig. 5B–D).

5. Discussion

5.1. Mechanisms for the expansion of Xiaojiang River watershed

Strike-slip faulting accommodates predominantly lateral shear displacement and produces fault damage zones characterized by extensive rock fragmentation (Kim et al., 2004; Mitchell and Faulkner, 2009; Savage and Brodsky, 2011; Rempe et al., 2013; Song et al., 2020; Wu et al., 2021). Within these zones, fractured bedrock exhibits reduced rock strength, making it more susceptible to weathering and fluvial erosion (Molnar et al., 2007; Roy et al., 2016; Zhang et al., 2026a). In the Xiaojiang River watershed, the main trunk channel follows the trace of the Xiaojiang Fault, whereas tributaries are oriented approximately perpendicular to it, underscoring the dominant structural control of strike-slip faulting on drainage network geometry (Figs. 1 and 2) (Roy et al., 2015). Moreover, the reduced bedrock strength within the fault damage zone likely enhances channel incision and headward erosion, thereby promoting outward migration of the drainage divide surrounding the Xiaojiang River watershed (Fig. 3). A representative example is the Jianshan River, a tributary of the Xiaojiang River, which is actively expanding into the adjacent Yili River watershed (Figs. 3 and 4). At present, the main stem of the Yili River lies only ~2 km from the headwaters of the Jianshan River, and the pronounced topographic contrast across the drainage divide indicates that the landscape is in a state of geomorphic disequilibrium (Fig. 4). Based on the current

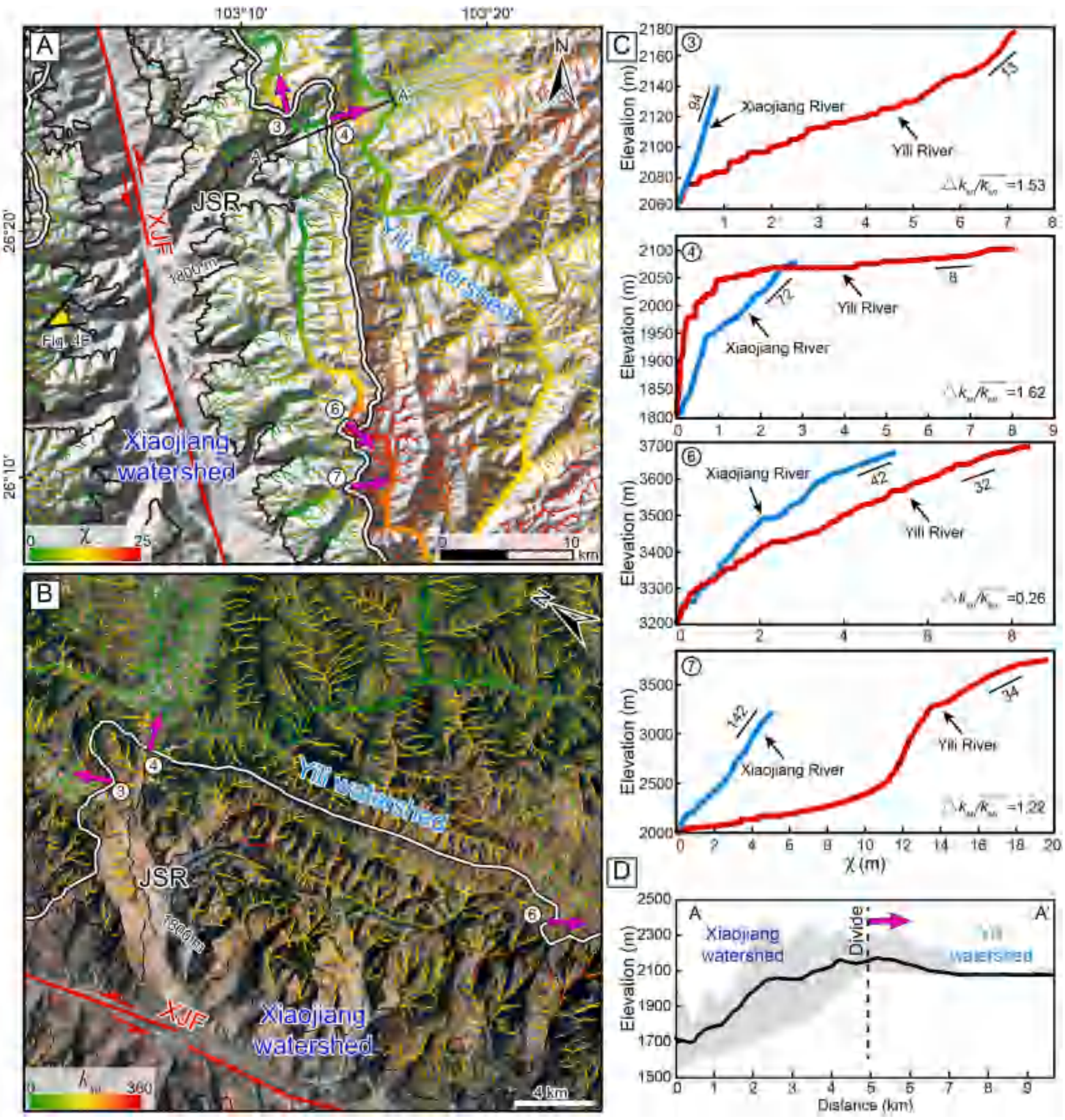

Fig. 4. (A) χ map with a base level elevation of 1800 m along the eastern flank of the Xiaojiang River watershed. The "eye" symbol depicts the viewing direction of the landscape shown in Panel B. (B) Perspective views of Google Earth image mapped with k_{sn} -analysis river channels. The topography on the western side is steeper than that on the eastern side. (C) χ plots for four pairs of river channels across the divide. Blue lines represent channels within in the Xiaojiang River watershed (aggressors) and red lines represent channels within the Yili River watershed (victims). The underlined numbers in the χ plots are the average k_{sn} values. (D) Swath profile with 2 km width along A-A′. The drainage divide is migrating toward the Yili River watershed. JSR: Jianshan River. (For interpretation of the references to colour in this figure legend, the reader is referred to the web version of this article.)

geomorphic configuration and observed patterns of divide migration, the Jianshan River appears likely to eventually capture the Yili River. However, the timing of such a capture event remains highly uncertain as divide migration rates are poorly constrained and may vary over time in response to changes in tectonic activity, climate, and other geomorphic processes.

In addition to weakened bedrock, strike-slip faulting along the Xiaojiang Fault induces an asymmetric local base-level response within the Xiaojiang River watershed (Ye et al., 2025). Owing to long-term sinistral displacement, tributary confluences on the eastern flank have been shifted downstream along the trunk channel, lowering the local base levels. This base-level fall further intensifies fluvial incision and headward erosion on the eastern flank, thereby favoring eastward divide migration. Conversely, upstream displacement of tributary confluences

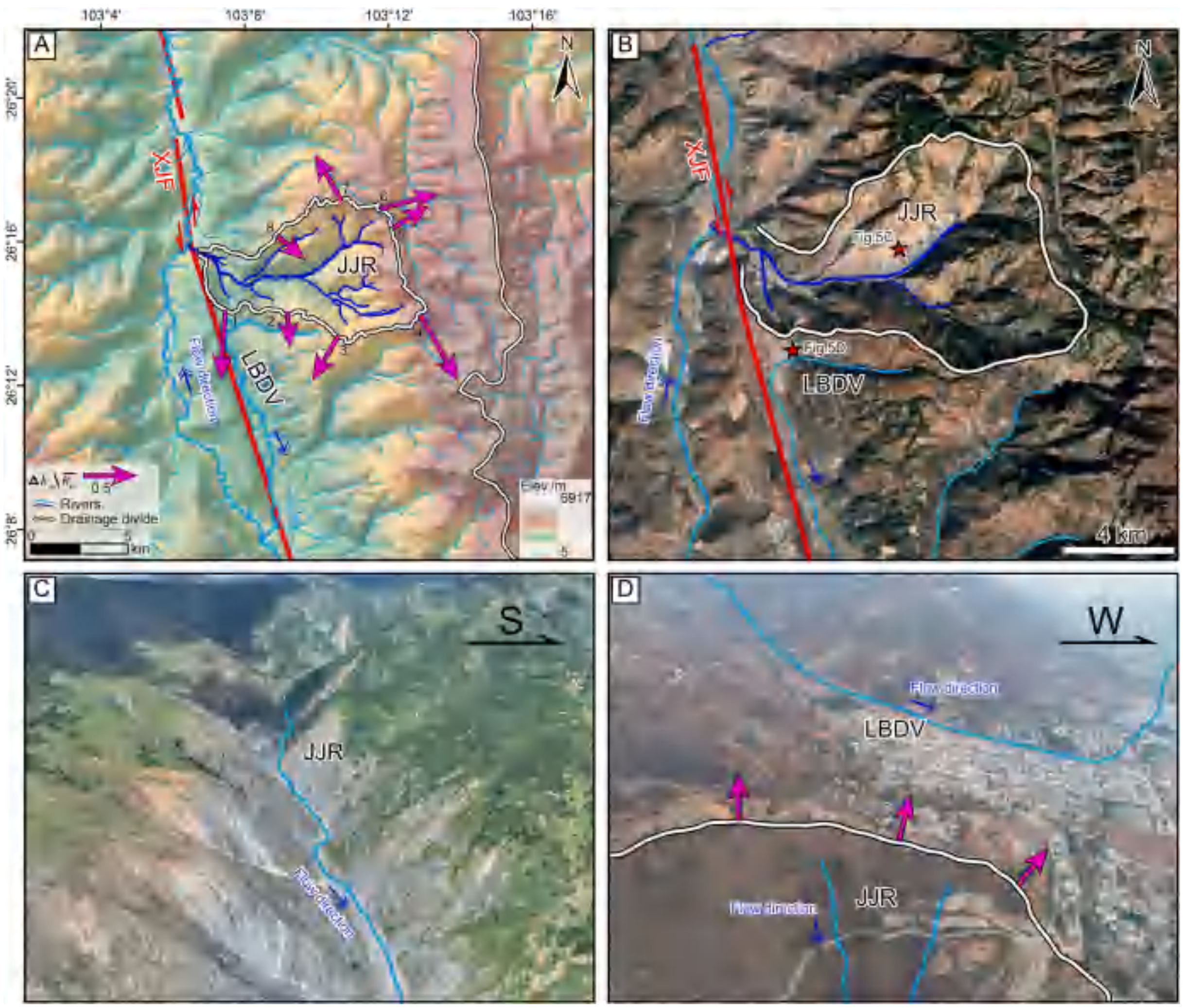

Fig. 5. (A) Stability of the drainage divide surrounding the Jiangjia Ravine. The vectors in magenta represent the migration direction and normalized cross-divide difference in k_{sn} ($\Delta k_{sn}/\overline{k_{sn}}$). The Jiangjia Ravine is expanding into the surrounding catchments. The detailed results of the χ plots are provided in Supplementary Materials Fig. S2 and Table S2. (B) Google Earth imagery. The stars indicate the location of the Panel C and D. (C—D) Field survey photographs. Geohazards are more prevalent in the Jiangjia Ravine than in the Laobaidi Valley. JJR: Jiangjia Ravine; LBDV: Laobaidi Valley. (For interpretation of the references to colour in this figure legend, the reader is referred to the web version of this article.)

on the western flank has resulted in localized base-level rise, reducing erosional efficiency and leading to drainage contraction in some headwater tributaries (Fig. 3).

Tectonic uplift has been shown to drive drainage reorganization across the southeastern Tibetan Plateau, primarily manifested by a progressive shift from southward- to eastward-flowing rivers (Clark et al., 2005; Tian et al., 2015; Zhou et al., 2022b; Ye et al., 2024a; Cao et al., 2025). However, all major rivers in the study area flow predominantly northward. Alternatively, if the Xiaojiang River watershed had experienced lower uplift rates than the adjacent catchments to the east and west, differential uplift could also have promoted the expansion of the Xiaojiang River watershed. However, recent thermochronological data indicate that both sides of the Xiaojiang Fault have experienced balanced uplift since 13 Ma (Zhang et al., 2026b). Therefore, although tectonic uplift has enhanced the fluvial incision, it cannot adequately explain the observed expansion of the Xiaojiang River watershed.

We also evaluated the potential influences of climate and lithology. Precipitation gradients can influence drainage-divide migration by producing differences in erosional efficiency between neighboring catchments (Bonnet, 2009; Bian et al., 2024; Gao et al., 2025). In this region, precipitation is higher to the east of the Xiaojiang River watershed (Fig. 2B), a pattern that would tend to drive divide migration toward the drier Xiaojiang River watershed—opposite to the observed eastward migration of the drainage divide. Lithologic contrasts likewise do not appear to exert a first-order control, as variations in bedrock type across drainage divides show no systematic relationship with migration direction (Figs. 2A and 3).

Collectively, these observations suggest that regional uplift, precipitation, and lithology may modulate the course of drainage evolution but are insufficient to explain the spatial pattern of drainage expansion and contraction documented here. Instead, sinistral strike-slip deformation along the Xiaojiang Fault offers the most consistent explanation, as it simultaneously account for both the widespread catchment expansion through fault-related bedrock weakening and the contrasting drainage evolution of the eastern and western flanks through asymmetric base-level adjustment.

5.2. Drainage-divide migration impacts regional geohazards

The spatial distribution of landslides within the Xiaojiang River watershed closely corresponds to the patterns of drainage-network evolution: expanding catchments generally exhibit higher landslide densities, whereas shrinking basins contain comparatively fewer landslides (Fig. 6). In rapidly expanding catchments, river channels show

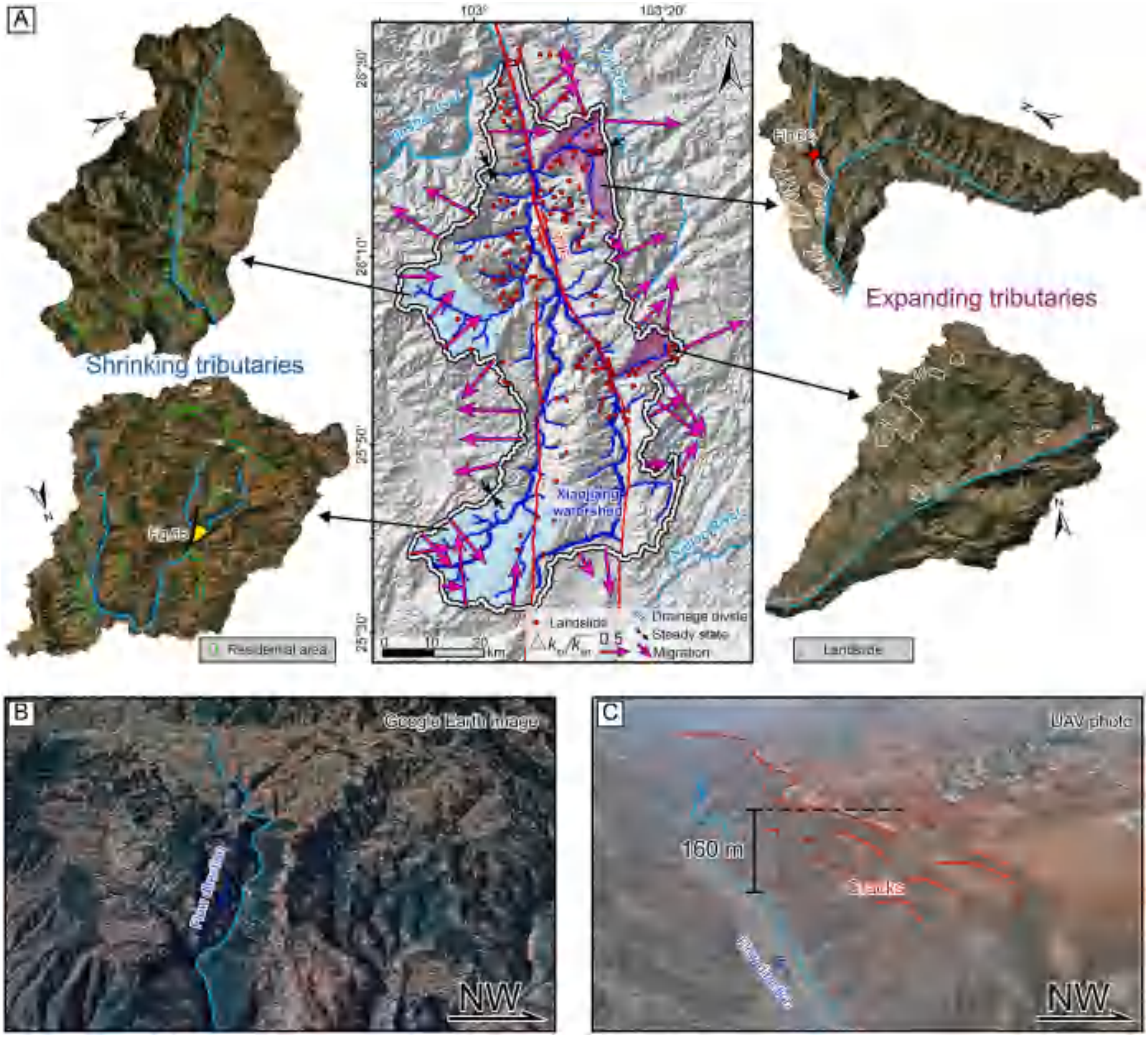

Fig. 6. (A) Landslides distribution in the Xiaojiang River watershed and three-dimensional perspective view of the shrinking and expanding basins. The expanding catchments (aggressive catchments) exhibit significantly higher landslide densities than shrinking basins (victim catchments). The green circles represent the inhabited areas. The white circles indicate the areas of slope instability. The "eye" symbol depicts the viewing direction of the landscape shown in Panel B. The stars indicate the location of the Panel C. (B) Google Earth imagery of the shrinking basin. The basin exhibits a lower landslide density, supporting large human populations. (C) UAV photo of the expanding basin. River incision depth reaches up to ~160 m. (For interpretation of the references to colour in this figure legend, the reader is referred to the web version of this article.)

incision depths of up to ~160 m, indicating substantial fluvial downcutting and active geomorphic adjustment (Fig. 6C).

Strike-slip faulting along the Xiaojiang Fault enhances fluvial erosion through both the fault-related bedrock weakening and base-level adjustment, thereby promoting divide migration and catchment expansion. As expanding basins progressively capture additional drainage area, the resulting increase in discharge and stream power may further enhance fluvial erosional capacity, establishing a positive feedback in which enhanced incision promotes further divide migration and drainage reorganization (Willett et al., 2014; Whipple et al., 2017). Sustained channel incision increases local relief and triggers hillslope adjustment, raising susceptibility to slope failure as gradients approach or exceed critical thresholds (Ouimet et al., 2009; Burbank et al., 1996). Beyond its effects on channel processes, fault-related fracturing can directly weaken hillslope bedrock and create structural discontinuities, further reducing slope stability. Collectively, these tectonically driven processes create favorable geomorphic conditions for landslide occurrence within expanding catchments, where hillslopes are continuously adjusting to enhanced river incision (Burbank et al., 1996; Montgomery, 2001; Montgomery and Brandon, 2002; Larsen and Montgomery, 2012).

While tectonic deformation and river incision set the long-term conditions for hillslope instability, short-term perturbations—such as intense rainfall and earthquake shaking—may act as immediate triggers for slope failures in expanding drainage basins. Moreover, landslide-derived sediment can modulate the efficiency of channel incision, either by supplying abrasive tools for bedrock erosion or by promoting transient channel aggradation. Through their influence on sediment transport and channel dynamics, these hillslope-channel feedbacks may in turn affect long-term drainage evolution and divide migration, although their relative importance remains to be quantified.

Overall, these observations suggest that drainage evolution and catchment-scale geomorphic adjustment play an important role in shaping the spatial pattern of geohazards within the Xiaojiang River watershed. Expanding basins exhibit enhanced geomorphic adjustment, where higher landslide densities likely reflect intensified channel incision and associated topographic disequilibrium (Fig. 6A and C). In contrast, shrinking basins progressively lose contributing area, which reduces drainage area, discharge and channel erosional capacity, thereby limiting channel incision and contributing to comparatively lower landslide activity (Fig. 6A and B).

5.3. Strike-slip faulting drives the internal drainage reorganization

Strike-slip faulting can progressively offset and elongate river channels oriented perpendicular to the fault trace (Hubert-Ferrari et al., 2002; Ouchi, 2005; Duvall and Tucker, 2015; Tian and Lin, 2021; Aránguiz-Rago et al., 2025). Continued fault slip frequently leads to drainage reorganization through divide migration and stream capture (Duvall and Tucker, 2015; Zeng and Tan, 2023). On the eastern flank of the Xiaojiang River watershed, the drainage network exhibits anomalous planform geometry: the river channels within the Laobaidi Valley flow southward for approximately 11 km across a low-relief surface before making an abrupt bend to join the north-flowing Xiaojiang trunk stream (Fig. 5A). Combining these observations with the drainage-divide stability analysis of the Jiangjia Ravine (Fig. 5), we propose an evolutionary model of tectonically driven drainage reorganization in the eastern Xiaojiang River watershed in response to the sinistral strike-slip displacements along the Xiaojiang Fault.

Before substantial fault-driven channel elongation occurred (~1.1–1.8 Ma, estimated from fault slip rates and channel offset), eastern tributaries drained directly into the main channel of the Xiaojiang River (Fig. 7A). Progressive sinistral displacement along the Xiaojiang Fault subsequently offset tributary channels, progressively elongating river channels in both the Jiangjia Ravine and Laobaidi Valley (Fig. 7B). This fault-induced channel elongation increased the steady-state elevations of the river channels, making the affected channels increasingly susceptible to capture by adjacent streams (Willett et al., 2014; Ye et al., 2024b). Continued divide migration ultimately enabled the capture of the paleo-Jiangjia River by a neighboring captor river, resulting in a substantial local base-level fall that enhanced channel incision and promoted further basin expansion (Fig. 7C). Although geomorphic evidence supports the occurrence of this river-capture event, its timing remains poorly constrained because quantitative estimates of erosion coefficients and independent chronological constraints are currently unavailable. Future integration of geomorphic analyses with chronological data will help constrain the timing of river capture and refine the evolutionary history of the Xiaojiang River watershed.

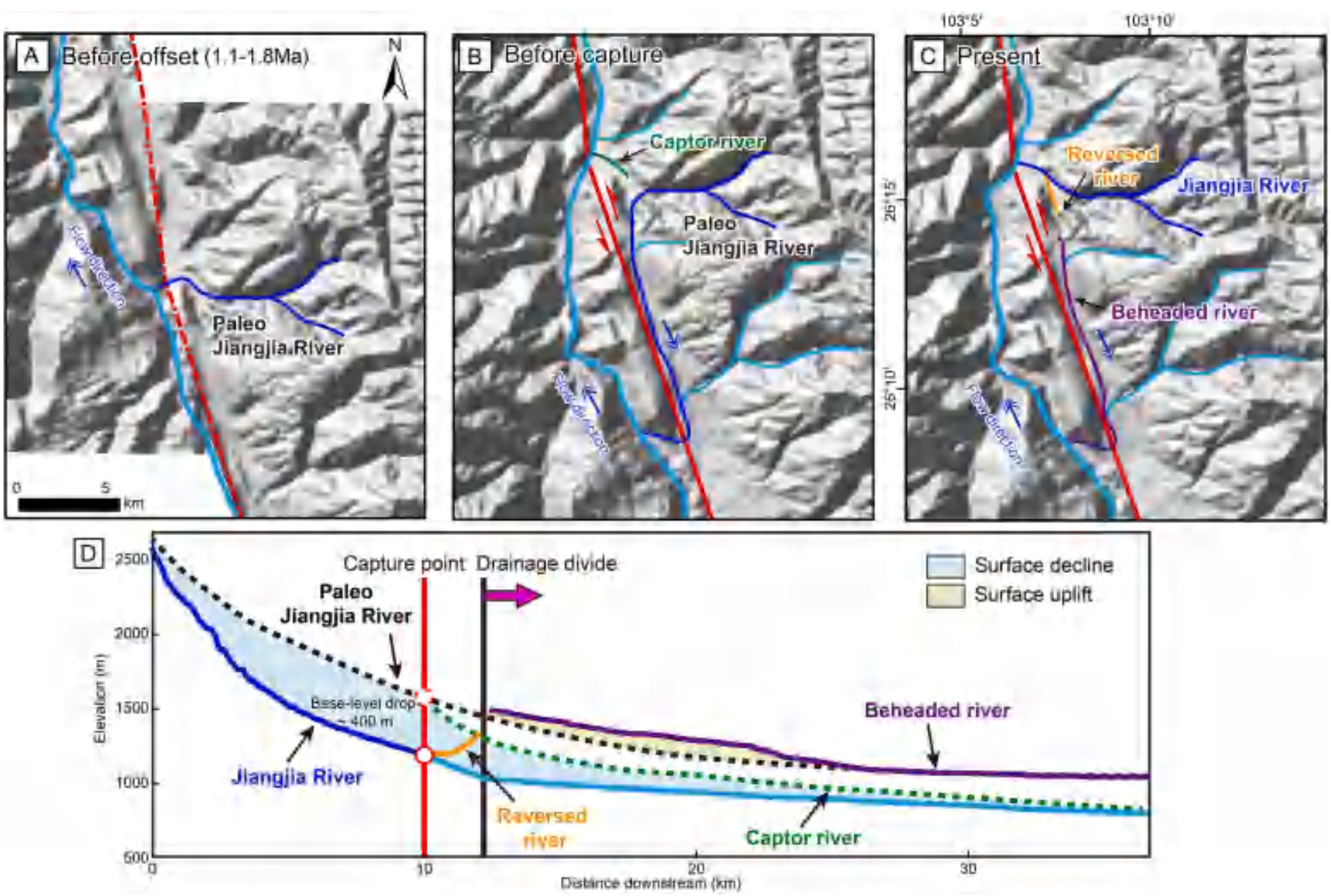

Fig. 7. Diagrams of drainage evolution driven by strike-slip faulting. (A) Before significant fault-driven channel offset (1.1–1.8 Ma), eastern tributaries flowed directly into the main channel of the Xiaojiang River. This timescale is estimated based on the late Quaternary slip rate of the eastern Xiaojiang Fault and the observed ~11 km elongation of the Laobaidi Valley river channel. It represents the duration required for cumulative sinistral displacement to produce the observed channel configuration and geomorphic disequilibrium, rather than the precise timing of the river-capture event. (B) Sinistral strike-slip motion offset and elongated the river channels. (C) The Jiangjia River has been captured by the neighboring river channel. The base-level fall enhanced erosion rates and facilitated basin expansion. (D) Schematic of the model scenario for post-capture profile incision. The solid light blue curve indicates the modern Jiangjia River profile, the solid purple curve indicates the modern beheaded river, and the solid orange curve indicates the reversed river channel. The dashed black curve indicates the Paleo-Jiangjia River and the dashed green curve indicates the captor river. The red vertical bar represents the capture point and the black vertical bar represents the location of the modern drainage divide. The blue area on the profile represents the decline of river channel, whereas the yellow area represents the uplift. (For interpretation of the references to colour in this figure legend, the reader is referred to the web version of this article.)

5.4. Sudden fall of erosional base level triggered geohazards in Jiangjia Ravine

River capture can reorganize fluvial networks by shortening channel lengths and modifying sediment-routing pathways (Bishop, 1995; Duvall and Tucker, 2015). Such perturbations commonly induce a sharp local base-level fall at and upstream of the capture point, triggering enhanced channel incision and the upstream knickpoint migration (Whipple and Tucker, 1999; Gallen et al., 2011; Fan et al., 2018). During this transient adjustment phase, increased incision may destabilize adjacent hillslopes, promoting slope failures and debris-flow activity (Burbank et al., 1996; Bigi et al., 2006; Ng, 2006; Korup and Schlunegger, 2007; Reinhardt et al., 2007; Gallen et al., 2011; Larsen and Montgomery, 2012; Baynes et al., 2022). In addition, drainage capture increases contributing area and discharge within the captor river, which can further enhance river downcutting and soil erosion. Collectively, these processes provide a plausible mechanistic framework for interpreting the elevated geohazard activity observed in the Jiangjia Ravine.

In the study area, capture of the paleo-Jiangjia River is inferred to have produced an estimated ~400 m drop in local erosional base level, based on present-day topography and reconstruction of the pre-capture longitudinal river profile (Fig. 7D). This magnitude of base-level change would be expected to promote rapid channel incision and associated hillslope destabilization. Consistent with this interpretation, the Jiangjia Ravine has experienced a pronounced concentration of geohazard activity, with 278 documented debris-flow events between 1961 and 2004 (Wei et al., 2025), whereas no comparable debris-flow records have been reported from the adjacent Laobaidi Valley, which has not been captured (Figs. 5 and 6). Given the close proximity of the two basins, contrasts in lithology and precipitation are limited (Figs. 2 and 5B). The spatial correspondence between capture-driven incision and concentrated geohazard occurrence therefore suggests that drainage reorganization (i.e., river capture) has played an important role in controlling recent landscape instability in this region.

Ongoing divide migration in the Jiangjia Ravine suggests that additional river capture involving the Laobaidi Valley tributaries may occur, indicating that drainage reorganization on the eastern flank of the Xiaojiang River watershed remains an active process (Figs. 5 and 7). Continued evolution of the drainage network may further modify local base levels, discharge distribution, and sediment-routing pathways in the Laobaidi Valley, with potential implications for future geohazard activity. The Xiaojiang River watershed provides a distinctive example of how active strike-slip faulting, drainage reorganization, and the geohazard distribution are dynamically coupled through long-term landscape evolution. More broadly, this case study suggests that, in tectonically active mountain belts, drainage reorganization is not merely a passive response to tectonic forcing but also an active process that modulates erosion patterns and influences the spatial distribution of geohazards. Incorporating dynamic drainage evolution into regional hazard-assessment frameworks is therefore essential for understanding landscape adjustment and improving long-term geohazard risk assessment.

6. Conclusions

We measured the drainage-divide stability in the Xiaojiang River watershed using χ-plots analysis. Combined with field investigation and quantitative topographic analyses, we evaluated the controls on drainage reorganization and their implications for the spatial distribution of geohazards in the Xiaojiang River watershed. The principal findings are as follows:

(1) The Xiaojiang River watershed is undergoing widespread catchment expansion, primarily controlled by fault-related bedrock weakening associated with the Xiaojiang Fault. This expansion is especially pronounced among the eastern tributaries, where long-term sinistral strike-slip displacement has shifted tributary confluences downstream along the trunk channel, thereby enhancing fluvial incision and driving eastward divide migration.

(2) Geohazards are more densely distributed within expanding tributary basins than within shrinking basins. This spatial relationship indicates that drainage evolution—particularly changes in watershed boundaries—plays an important role in governing the distribution of geohazards.

(3) At the sub-basin scale, the Jiangjia Ravine has experienced a river-capture event driven by the sinistral strike-slip motion along the Xiaojiang Fault. This capture induced an abrupt local base-level fall of ~400 m, accelerating channel incision and contributing to the development of severe geohazards in the Jiangjia Ravine.

CRediT authorship contribution statement

Yijia Ye: Writing – review & editing, Writing – original draft, Software, Methodology, Investigation, Formal analysis. **Xibin Tan:** Writing – review & editing, Validation, Supervision, Software, Funding acquisition, Formal analysis, Data curation, Conceptualization. **Dongri Song:** Writing – review & editing, Data curation.

Declaration of competing interest

The authors declare that they have no known competing financial interests or personal relationships that could have influenced the work reported in this paper.

Acknowledgments

This study is supported by the CAS Pioneer Hundred Talents Program (E2K2010010) and China Postdoctoral Science Foundation (2025M770425). We appreciate the constructive suggestions from the two anonymous reviewers, which substantially improved the manuscript.

Appendix A. Supplementary data

Supplementary data to this article can be found online at https://doi.org/10.1016/j.catena.2026.110529.

Data availability

The data obtained in this study can be acquired from doi:https://doi.org/10.6084/m9.figshare.32252046. The topography data (ALOS digital elevation models) were obtained from the Alaska Satellite Facility Data Search (https://search.asf.alaska.edu/). The precipitation data were downloaded from https://data.biogeo.ucdavis.edu/data/worldclim/v2.1/base/wc2.1_30s_prec.zip.

References

Aránguiz-Rago, T.F., Duvall, A.R., Crowell, B.W., Henderson, S.T., Schmidt, D.A., 2025. Slow strike-slip faulting in a hyper-arid landscape: assessing the geomorphic response to the Salar Grande Fault, Atacama Desert, Chile. J. Geophys. Res. Earth Surf. 130, e2024JF008018. https://doi.org/10.1029/2024JF008018.

Bai, Z., Shi, X., Chen, H., Shu, Y., Wang, J., Liu, X., Xu, C., Hilley, G., 2025. Consistent cumulative slip rates but shifting fault strand activity in the Xiaojiang Fault Zone, Southeastern Tibetan Plateau, across decadal and millennial timescales. Tectonics 44, e2025TC008905. https://doi.org/10.1029/2025TC008905.

Baynes, E.R.C., Lague, D., Steer, P., Davy, P., 2022. Dynamic bedrock channel width during knickpoint retreat enhances undercutting of coupled hillslopes. Earth Surf. Process. Landf. 47, 3629–3640. https://doi.org/10.1002/esp.5477.

Beeson, H.W., McCoy, S.W., Keen-Zebert, A., 2017. Geometric disequilibrium of river basins produces long-lived transient landscapes. Earth Planet. Sci. Lett. 475, 34–43. https://doi.org/10.1016/j.epsl.2017.07.010.

Bian, S., Tan, X., Liu, Y., Fan, S., Gong, J., Zhou, C., Shi, F., Murphy, M.A., 2024. Orographic rainfall drives the Himalaya drainage divide to move north. Geomorphology 444, 108952. https://doi.org/10.1016/j.geomorph.2023.108952.

Bian, S., Tan, X., Zuza, A.V., Zhou, C., Shi, F., Liu, Y., Gong, J., 2025. How does the newly-formed drainage divide migrate after a river capture event? Earth Planet. Sci. Lett. 651, 119165. https://doi.org/10.1016/j.epsl.2024.119165.

Bigi, A., Hasbargen, L.E., Montanari, A., Paola, C., 2006. Knickpoints and hillslope failures: interactions in a steady-state experimental landscape. In: Tectonics, Climate, and Landscape Evolution. Geological Society of America. https://doi.org/10.1130/2006.2398(18).

Bishop, P., 1995. Drainage rearrangement by river capture, beheading and diversion. Prog. Phys. Geog. Earth Environ. 19, 449–473. https://doi.org/10.1177/030913339501900402.

Blöthe, J.H., Korup, O., Schwanghart, W., 2015. Large landslides lie low: excess topography in the Himalaya-Karakoram ranges. Geology 43, 523–526. https://doi.org/10.1130/G36527.1.

Bonnet, S., 2009. Shrinking and splitting of drainage basins in orogenic landscapes from the migration of the main drainage divide. Nat. Geosci. 2, 766–771. https://doi.org/10.1038/ngeo666.

Burbank, D.W., Leland, J., Fielding, E., Anderson, R.S., Brozovic, N., Reid, M.R., Duncan, C., 1996. Bedrock incision, rock uplift and threshold hillslopes in the northwestern Himalayas. Nature 379, 505–510. https://doi.org/10.1038/379505a0.

Cao, K., Wang, G., Harrison, T.M., Yuan, X., Leloup, P.H., Kusky, T.M., Cao, L., Shen, X., Cheng, Y., Yao, J., He, X., Zhu, Z., Xie, S., 2025. Late Cenozoic river reorganization related to tectonic extrusion formed the modern drainage system in southeastern Tibet. Proc. Natl. Acad. Sci. USA 122. https://doi.org/10.1073/pnas.2424554122.

Chen, C.-Y., Willett, S.D., Christl, M., Shyu, J.B.H., 2021a. Drainage basin dynamics during the transition from early to mature orogeny in southern Taiwan. Earth Planet. Sci. Lett. 562, 116874. https://doi.org/10.1016/j.epsl.2021.116874.

Chen, Z., Zhou, H., Ye, F., Liu, B., Fu, W., 2021b. The characteristics, induced factors, and formation mechanism of the 2018 Baige landslide in Jinsha River, Southwest China. Catena 203, 105337. https://doi.org/10.1016/j.catena.2021.105337.

Chen, Q., Song, D., Chen, X., Zhong, W., 2023. Visco-collisional scaling law of flow resistance and its application in debris-flow mobility. J. Geophys. Res.: Earth Surf. 128, e2022JF006712. https://doi.org/10.1029/2022JF006712.

Clark, M.K., House, M.A., Royden, L.H., Whipple, K.X., Burchfiel, B.C., Zhang, X., Tang, W., 2005. Late Cenozoic uplift of southeastern Tibet. Geology 33 (6), 525–528. https://doi.org/10.1130/G21265.1.

Cui, P., Chen, X., Waqng, Y., Hu, K., Li, Y., 2005. Jiangjia Ravine debris flows in southwestern China. In: Debris-Flow Hazards and Related Phenomena. Springer Berlin Heidelberg, Berlin, Heidelberg, pp. 565–594.

Dascher-Cousineau, K., Finnegan, N.J., Brodsky, E.E., 2021. The life span of fault-crossing channels. Science 373, 204–207. https://doi.org/10.1126/science.abf2320.

Duffy, O.B., Brocklehurst, S.H., Gawthorpe, R.L., Leeder, M.R., Finch, E., 2015. Controls on landscape and drainage evolution in regions of distributed normal faulting: Perachora Peninsula, Corinth Rift, Central Greece. Basin Res. 27, 473–494. https://doi.org/10.1111/bre.12084.

Duvall, A.R., Tucker, G.E., 2015. Dynamic ridges and valleys in a strike-slip environment. J. Geophys. Res. Earth Surf. 120, 2016–2026. https://doi.org/10.1002/2015JF003618.

Fan, N., Chu, Z., Jiang, L., Hassan, M.A., Lamb, M.P., Liu, X., 2018. Abrupt drainage basin reorganization following a Pleistocene river capture. Nat. Commun. 9, 3756. https://doi.org/10.1038/s41467-018-06238-6.

Forte, A.M., Whipple, K.X., 2018. Criteria and tools for determining drainage divide stability. Earth Planet. Sci. Lett. 493, 102–117. https://doi.org/10.1016/j.epsl.2018.04.026.

Forte, A.M., Whipple, K.X., 2019. Short communication: the Topographic Analysis Kit (TAK) for TopoToolbox. Earth Surf. Dyn. 7, 87–95. https://doi.org/10.5194/esurf-7-87-2019.

Gallen, S.F., Wegmann, K.W., Frankel, K.L., Hughes, S., Lewis, R.Q., Lyons, N., Paris, P., Ross, K., Bauer, J.B., Witt, A.C., 2011. Hillslope response to knickpoint migration in the southern Appalachians: implications for the evolution of post-orogenic landscapes. Earth Surf. Process. Landf. 36, 1254–1267. https://doi.org/10.1002/esp.2150.

Gao, F., Tan, X., Zhou, C., Bian, S., Shi, F., 2025. Eastward drainage-divide migrations driven by the spatial variations in precipitation and tectonic uplift contribute to the formation of the parallel rivers in the Hengduan Mountains, Southeastern Tibet. Geomorphology 468, 109513. https://doi.org/10.1016/j.geomorph.2024.109513.

Gray, H.J., Shobe, C.M., Hobley, D.E.J., Tucker, G.E., Duvall, A.R., Harbert, S.A., Owen, L.A., 2018. Off-fault deformation rate along the southern San Andreas fault at Mecca Hills, southern California, inferred from landscape modeling of curved drainages. Geology 46, 59–62. https://doi.org/10.1130/G39820.1.

Guo, P., Han, Z., Dong, S., Mao, Z., Hu, N., Gao, F., Li, J., 2021. Latest quaternary active faulting and paleoearthquakes on the southern segment of the Xiaojiang fault zone, SE Tibetan Plateau. Lithosphere 2021, 7866379. https://doi.org/10.2113/2021/7866379.

Harel, E., Goren, L., Shelef, E., Ginat, H., 2019. Drainage reversal toward cliffs induced by lateral lithologic differences. Geology 47, 928–932. https://doi.org/10.1130/G46353.1.

He, H., Oguchi, T., 2008. Late quaternary activity of the Zemuhe and Xiaojiang faults in southwest China from geomorphological mapping. Geomorphology 96, 62–85. https://doi.org/10.1016/j.geomorph.2007.07.009.

He, H.L., Fang, Z.J., Li, P., 1993. A preliminary approach to the fault activity of southern segment on Xiaojiang west branch fault. J. Seismol. Res. 16 (3), 291–298.

He, H.L., Yasutaka, I., Song, F.M., Dong, X.Q., 2002. Late quaternary slip rate of the Xiaojiang fault and its implication. Seismol. Geol. 24 (1), 14–26.

Howard, A.D., 1994. A detachment-limited model of drainage basin evolution. Water Resour. Res. 30, 2261–2285. https://doi.org/10.1029/94WR00757.

Hu, K., Wei, F., Li, Y., 2011. Real-time measurement and preliminary analysis of debris-flow impact force at Jiangjia Ravine, China: real-time measurement and analysis of debris-flow impact force. Earth Surf. Process. Landf. 36, 1268–1278. https://doi.org/10.1002/esp.2155.

Hu, M., Wu, Z., Reicherter, K., Ali, S., Huang, X., Zuo, J., 2021. A historical earthquake-induced landslide damming event at the Qiaojia Reach of the Jinsha River, SE Tibetan Plateau: implication for the seismic hazard of the Xiaojiang Fault. Front. Earth Sci. 9, 649543. https://doi.org/10.3389/feart.2021.649543.

Hubert-Ferrari, A., Armijo, R., King, G., Meyer, B., Barka, A., 2002. Morphology, displacement, and slip rates along the North Anatolian Fault, Turkey. J. Geophys. Res. Solid Earth 107, ETG 9-1–ETG 9-33. https://doi.org/10.1029/2001JB000393.

Kim, Y.-S., Peacock, D.C.P., Sanderson, D.J., 2004. Fault damage zones. J. Struct. Geol. 26, 503–517. https://doi.org/10.1016/j.jsg.2003.08.002.

Kirby, E., Whipple, K.X., 2012. Expression of active tectonics in erosional landscapes. J. Struct. Geol. 44, 54–75. https://doi.org/10.1016/j.jsg.2012.07.009.

Kirby, E., Whipple, K.X., Tang, W., Chen, Z., 2003. Distribution of active rock uplift along the eastern margin of the Tibetan Plateau: inferences from bedrock channel longitudinal profiles. J. Geophys. Res. https://doi.org/10.1029/2001JB000861.

Korup, O., Schlunegger, F., 2007. Bedrock landsliding, river incision, and transience of geomorphic hillslope-channel coupling: evidence from inner gorges in the Swiss Alps. J. Geophys. Res. 112, 2006JF000710. https://doi.org/10.1029/2006JF000710.

Lan, H.X., Zhou, C.H., Wang, L.J., Zhang, H.Y., Li, R.H., 2004. Landslide hazard spatial analysis and prediction using GIS in the Xiaojiang watershed, Yunnan, China. Eng. Geol. 76, 109–128. https://doi.org/10.1016/j.enggeo.2004.06.009.

Larsen, I.J., Montgomery, D.R., 2012. Landslide erosion coupled to tectonics and river incision. Nat. Geosci. 5, 468–473. https://doi.org/10.1038/ngeo1479.

Li, Y., Chen, J., Yan, J., Zhou, F., Wang, Q., Li, Z., Zhang, Y., 2022. Formation and evolution of a giant old deposit in the First Bend of the Yangtze River on the southeastern margin of the Qinghai-Tibet Plateau. CATENA 213, 106138. https://doi.org/10.1016/j.catena.2022.106138.

Li, H., Yuan, D., Su, Q., Si, G., Wen, Y., Chen, Y., 2025. Drainage divides migration of the Heihe River in the Qilian Mountains, northeastern Tibet: insights for the drainage reorganization in an orogenic belt. Earth Surf. Process. Landf. 50, e70084. https://doi.org/10.1002/esp.70084.

Min, Z.Q., Wu, G., Jiang, Z.X., Liu, C.S., Yang, Y.L., 1995. Catalog of Chinese Historic Strong Earthquakes from BC 2300 to AD 1911. Seismological Publishing Press, Beijing.

Mitchell, T.M., Faulkner, D.R., 2009. The nature and origin of off-fault damage surrounding strike-slip fault zones with a wide range of displacements: a field study from the Atacama fault system, northern Chile. J. Struct. Geol. 31, 802–816. https://doi.org/10.1016/j.jsg.2009.05.002.

Molnar, P., Anderson, R.S., Anderson, S.P., 2007. Tectonics, fracturing of rock, and erosion. J. Geophys. Res. 112, 2005JF000433. https://doi.org/10.1029/2005JF000433.

Montgomery, D.R., 2001. Slope distributions, threshold hillslopes, and steady-state topography. Am. J. Sci. 301, 432–454. https://doi.org/10.2475/ajs.301.4-5.432.

Montgomery, D.R., Brandon, M.T., 2002. Topographic controls on erosion rates in tectonically active mountain ranges. Earth Planet. Sci. Lett. 201, 481–489. https://doi.org/10.1016/S0012-821X(02)00725-2.

Morales, B., Lizama, E., Somos-Valenzuela, M., Rivera, D., Ningshen, C., 2023. Earthquake-induced landslides coupled to fluvial incision in Andean Patagonia: inferring their effects on landscape at geological time scales. Geomorphology 434, 108731. https://doi.org/10.1016/j.geomorph.2023.108731.

Ng, K.Y., 2006. Landslide locations and drainage network development: a case study of Hong Kong. Geomorphology 76, 229–239. https://doi.org/10.1016/j.geomorph.2005.10.008.

Ouchi, S., 2005. Development of offset channels across the San Andreas fault. Geomorphology 70, 112–128. https://doi.org/10.1016/j.geomorph.2005.04.004.

Ouimet, W.B., Whipple, K.X., Granger, D.E., 2009. Beyond threshold hillslopes: channel adjustment to base-level fall in tectonically active mountain ranges. Geology 37, 579–582. https://doi.org/10.1130/G30013A.1.

Pei, Y., Qiu, H., Yang, D., Liu, Z., Ma, S., Li, J., Cao, M., Wufuer, W., 2023. Increasing landslide activity in the Taxkorgan River Basin (eastern Pamirs Plateau, China) driven by climate change. CATENA 223, 106911. https://doi.org/10.1016/j.catena.2023.106911.

Perron, J.T., Royden, L., 2013. An integral approach to bedrock river profile analysis. Earth Surf. Process. Landf. 38, 570–576. https://doi.org/10.1002/esp.3302.

Qi, T., Meng, X., Zhao, Y., Li, Y., 2025. Ancient very large and giant landslides on the eastern margin of the Qinghai–Tibet Plateau, China. Eng. Geol. 346, 107889. https://doi.org/10.1016/j.enggeo.2024.107889.

Reinhardt, L.J., Bishop, P., Hoey, T.B., Dempster, T.J., Sanderson, D.C.W., 2007. Quantification of the transient response to base-level fall in a small mountain catchment: Sierra Nevada, southern Spain. J. Geophys. Res. 112, 2006JF000524. https://doi.org/10.1029/2006JF000524.

Rempe, M., Mitchell, T., Renner, J., Nippress, S., Ben-Zion, Y., Rockwell, T., 2013. Damage and seismic velocity structure of pulverized rocks near the San Andreas Fault. J. Geophys. Res. Solid Earth 118, 2813–2831. https://doi.org/10.1002/jgrb.50184.

Ren, Z., 2013. Geometry and deformation features of the most recent co-seismic surface ruptures along the Xiaojiang Fault and its tectonic implications for the Tibetan Plateau. J. Asian Earth Sci. 77, 21–30. https://doi.org/10.1016/j.jseaes.2013.08.016.

Roy, S.G., Koons, P.O., Upton, P., Tucker, G.E., 2015. The influence of crustal strength fields on the patterns and rates of fluvial incision. J. Geophys. Res. Earth Surf. 120, 275–299. https://doi.org/10.1002/2014JF003281.

Roy, S.G., Tucker, G.E., Koons, P.O., Smith, S.M., Upton, P., 2016. A fault runs through it: modeling the influence of rock strength and grain-size distribution in a fault-damaged landscape: rock strength, grain size, and erosion. J. Geophys. Res. Earth Surf. 121, 1911–1930. https://doi.org/10.1002/2015JF003662.

Savage, H.M., Brodsky, E.E., 2011. Collateral damage: evolution with displacement of fracture distribution and secondary fault strands in fault damage zones. J. Geophys. Res. 116, B03405. https://doi.org/10.1029/2010JB007665.

Schwanghart, W., Scherler, D., 2014. Short communication: TopoToolbox 2 – MATLAB-based software for topographic analysis and modeling in Earth surface sciences. Earth Surf. Dyn. 2, 1–7. https://doi.org/10.5194/esurf-2-1-2014.

Scott, K.M., Wang, Y., 2004. Debris Flows: Geologic Process and Hazard; Illustrated by a Surge Sequence at Jiangjia Ravine, Yunnan, China (No. 1671). US Geological Survey.

Shen, J., Yipeng, W., Fangmin, S., 2003. Characteristics of the active Xiaojiang fault zone in Yunnan, China: a slip boundary for the southeastward escaping Sichuan–Yunnan Block of the Tibetan Plateau. J. Asian Earth Sci. 21, 1085–1096. https://doi.org/10.1016/S1367-9120(02)00185-2.

Shen, Z., Lü, J., Wang, M., Bürgmann, R., 2005. Contemporary crustal deformation around the southeast borderland of the Tibetan Plateau. J. Geophys. Res. 110, 2004JB003421. https://doi.org/10.1029/2004JB003421.

Song, D., 2023. Analysis on the dynamic characteristics of debris flow in Jiangjia Ravine, China. E3S Web Conf. 415, 01023. https://doi.org/10.1051/e3sconf/202341501023.

Song, F.M., Wang, X.P., Yu, W.X., Gao, Z.Q., Shen, X.H., Shen, J., 1998. Xiaojiang Active Fault. Seimological Publishing Press, Beijing.

Song, W.J., Johnson, S.E., Gerbi, C.C., 2020. Quartz fluid inclusion abundance and off-fault damage in a deeply exhumed, strike-slip, seismogenic fault. J. Struct. Geol. 139, 104118. https://doi.org/10.1016/j.jsg.2020.104118.

Stokes, M.F., Larsen, I.J., Goldberg, S.L., McCoy, S.W., Prince, P.P., Perron, J.T., 2023. The erosional signature of drainage divide motion along the blue ridge escarpment. J. Geophys. Res. Earth Surf. 128, e2022JF006757. https://doi.org/10.1029/2022JF006757.

Sun, S., Liu, L., Hu, J., Ding, H., 2022. Failure characteristics and mechanism of a rain-triggered landslide in the northern longwall of Fushun west open pit, China. Landslides 19, 2439–2458. https://doi.org/10.1007/s10346-022-01926-3.

Tian, J., Lin, Z., 2021. Late quaternary activity of the Qingchuan Fault, eastern Tibetan Plateau margin: insights from stream channel offsets and catchment erosion. Geomorphology 395, 107949. https://doi.org/10.1016/j.geomorph.2021.107949.

Tian, Y., Kohn, B.P., Hu, S., Gleadow, A.J.W., 2015. Synchronous fluvial response to surface uplift in the eastern Tibetan Plateau: implications for crustal dynamics. Geophys. Res. Lett. 42, 29–35. https://doi.org/10.1002/2014GL062383.

Umar, Z., Pradhan, B., Ahmad, A., Jebur, M.N., Tehrany, M.S., 2014. Earthquake induced landslide susceptibility mapping using an integrated ensemble frequency ratio and logistic regression models in west Sumatera Province, Indonesia. CATENA 118, 124–135. https://doi.org/10.1016/j.catena.2014.02.005.

Wang, E., Burchfiel, B.C., 2000. Late Cenozoic to Holocene deformation in southwestern Sichuan and adjacent Yunnan, China, and its role in formation of the southeastern part of the Tibetan Plateau. GSA Bull. 112, 413–423. https://doi.org/10.1130/0016-7606(2000)112%253C413:LCTHDI%253E2.0.CO;2.

Wang, M., Shen, Z., 2020. Present-day crustal deformation of continental China derived from GPS and its tectonic implications. J. Geophys. Res. Solid Earth 125, e2019JB018774. https://doi.org/10.1029/2019JB018774.

Wang, E., Burchfiel, B.C., Royden, L.H., Chen, L.Z., Chen, J.S., Li, W.X., Chen, Z.L., 1998. Late Cenozoic Xianshuihe-Xiaojiang, Red River, and Dali fault systems of southwestern Sichuan and Central Yunnan, China. Geol. Soc. London Spec. Publ. 327, 1–108. https://doi.org/10.1130/0-8137-2327-2.1.

Wang, Y., Wang, E., Shen, Z., Wang, M., Gan, W., Qiao, X., Meng, G., Li, T., Tao, W., Yang, Y., Cheng, J., Li, P., 2008. GPS-constrained inversion of present-day slip rates along major faults of the Sichuan-Yunnan region, China. Sci. China Ser. D-Earth Sci. 51, 1267–1283. https://doi.org/10.1007/s11430-008-0106-4.

Wei, L., Song, D., Cui, P., Su, L., Zhou, G.G.D., Hu, K., Wei, F., Hong, Y., Ou, G., Zhang, J., Kang, Z., Guo, X., Zhong, W., Li, X., Zhang, Y., Shi, C., Tang, H., 2025. A long-term dataset of debris-flow and hydrometeorological observations from 1961 to 2024 in Jiangjia Ravine. China. Earth Syst. Sci. Data 17, 7331–7358. https://doi.org/10.5194/essd-17-7331-2025.

Wen, X., Du, F., Long, F., Fan, J., Zhu, H., 2011. Tectonic dynamics and correlation of major earthquake sequences of the Xiaojiang and Qujiang-Shiping fault systems, Yunnan, China. Sci. China Earth Sci. 54, 1563–1575. https://doi.org/10.1007/s11430-011-4231-0.

Whipple, K.X., Tucker, G.E., 1999. Dynamics of the stream-power river incision model: implications for height limits of mountain ranges, landscape response timescales, and research needs. J. Geophys. Res. 104, 17661–17674. https://doi.org/10.1029/1999JB900120.

Whipple, K.X., Forte, A.M., DiBiase, R.A., Gasparini, N.M., Ouimet, W.B., 2017. Timescales of landscape response to divide migration and drainage capture: implications for the role of divide mobility in landscape evolution. J. Geophys. Res. Earth Surf. 122, 248–273. https://doi.org/10.1002/2016JF003973.

Willett, S.D., McCoy, S.W., Perron, J.T., Goren, L., Chen, C.-Y., 2014. Dynamic reorganization of river basins. Science 343, 1248765. https://doi.org/10.1126/science.1248765.

Wobus, C., Whipple, K.X., Kirby, E., Snyder, N., Johnson, J., Spyropolou, K., Crosby, B., Sheehan, D., 2006. Tectonics from topography: procedures, promise, and pitfalls, in: tectonics, climate, and landscape evolution. Geol. Soc. Am. Spec. Pap. 398, 55–74. https://doi.org/10.1130/2006.2398(04).

Wu, C., Cui, P., Li, Y., Yi, S., 2021. Tectonic damage of crustal rock mass around active faults and its conceptual model at eastern margin of Tibetan Plateau. J. Eng. Geol. 29 (2), 289–306. https://doi.org/10.13544/j.cnki.jeg.2021-0075.

Yanites, B.J., Ehlers, T.A., Becker, J.K., Schnellmann, M., Heuberger, S., 2013. High magnitude and rapid incision from river capture: Rhine River, Switzerland. J. Geophys. Res. Earth Surf. 118, 1060–1084. https://doi.org/10.1002/jgrf.20056.

Ye, Y., Tan, X., Liu, Y., Bian, S., Zhou, C., Zeng, X., Shi, F., Gao, M., 2024a. Drainage reorganization and divide migration driven by basin subsidence: an example from the Micang Shan, outskirts of eastern Tibet and its implications for Cenozoic evolution of the Yangtze River. Basin Res. 36, e12875. https://doi.org/10.1111/bre.12875.

Ye, Y., Tan, X., Zhou, C., Bian, S., Liu, Y., Shi, F., 2024b. Cross-divide difference in channel-head steady-state elevation controls drainage-divide migration. Earth Surf. Process. Landf. 49, 3332–3343. https://doi.org/10.1002/esp.5892.

Ye, Y., Tan, X., Chen, C.-T., Liu, Y., Bian, S., Shi, F., 2025. Strike-Slip Faulting Drives Asymmetric Drainage Evolution of Rivers Draining Along the Fault. ESS Open Archive. https://doi.org/10.22541/essoar.175917138.88848813/v1.

Zeng, X., Tan, X., 2023. Drainage divide migration in response to strike-slip faulting: an example from northern Longmen Shan, eastern Tibet. Tectonophysics 848, 229720. https://doi.org/10.1016/j.tecto.2023.229720.

Zhang, J., Geng, H., Pan, B., Nie, J., Hu, X., Zhao, Q., Chen, D., Xie, R., 2022. Coupling of tectonic uplift and climate change as influences on drainage evolution: a case study at the NE margin of the Tibetan Plateau. Catena 216, 106433. https://doi.org/10.1016/j.catena.2022.106433.

Zhang, J., Zuo, X., Li, Y., Shi, M., Shi, C., Huang, C., Tang, X., 2025. Detection and assessment of potential landslides in the Xiaojiang River Basin using SBAS-InSAR. Sci. Rep. 15, 16082. https://doi.org/10.1038/s41598-025-00490-9.

Zhang, D., Dong, Y., Xie, Z., Yu, H., 2026a. Role of Cenozoic tectonic uplift in shaping the surface landscape of the Gongwang Shan, southeastern Tibetan Plateau. Palaeogeogr. Palaeoclimatol. Palaeoecol. 690, 113714. https://doi.org/10.1016/j.palaeo.2026.113714.

Zhang, G., Tian, Y., Li, J., Zuza, A.V., Zhang, B., Zhang, Z., Zhang, P., 2026b. Kinematic inversion of the Xianshuihe-Xiaojiang fault system from Oligocene shortening to late Miocene left-lateral slip in the southeastern Tibetan Plateau. GSA Bull. https://doi.org/10.1130/B38765.1.

Zhou, C., Tan, X., Liu, Y., Shi, F., 2022a. A cross-divide contrast index (C) for assessing controls on the main drainage divide stability of a mountain belt. Geomorphology 398, 108071. https://doi.org/10.1016/j.geomorph.2021.108071.

Zhou, C., Tan, X., Liu, Y., Lu, R., Murphy, M.A., He, H., Han, Z., Xu, X., 2022b. Ongoing westward migration of drainage divides in eastern Tibet, quantified from topographic analysis. Geomorphology 402, 108123. https://doi.org/10.1016/j.geomorph.2022.108123.

Zhuang, J., Cui, P., Wang, G., Chen, X., Iqbal, J., Guo, X., 2015. Rainfall thresholds for the occurrence of debris flows in the Jiangjia Gully, Yunnan Province, China. Eng. Geol. 195, 335–346. https://doi.org/10.1016/j.enggeo.2015.06.006.

Zondervan, J.R., Stokes, M., Boulton, S.J., Telfer, M.W., Mather, A.E., 2020. Rock strength and structural controls on fluvial erodibility: implications for drainage divide mobility in a collisional mountain belt. Earth Planet. Sci. Lett. 538, 116221. https://doi.org/10.1016/j.epsl.2020.116221.

Zou, Y., Qi, S., Guo, S., Zheng, B., Zhan, Z., He, N., Huang, X., Hou, X., Liu, H., 2022. Factors controlling the spatial distribution of coseismic landslides triggered by the Mw 6.1 Ludian earthquake in China. Eng. Geol. 296, 106477. https://doi.org/10.1016/j.enggeo.2021.106477.